

# $^1\text{H}$ and hyperpolarized $^3\text{He}$ magnetic resonance imaging clearly detect the preventative effect of a glucocorticoid on endotoxin-induced pulmonary inflammation *in vivo*

17(2) (2011) 204–211  
 © SAGE Publications 2010  
 ISSN 1753-4259 (print)  
 10.1177/1753425909359191

Lars E. Olsson<sup>1,2</sup>, Amir Smailagic<sup>3</sup>, Per-Ola Önnervik<sup>3</sup>, Anders Lindén<sup>4</sup>, Paul D. Hockings<sup>1</sup>

<sup>1</sup>DECS/Imaging, AstraZeneca R&D Mölndal, Mölndal, Sweden

<sup>2</sup>Department of Radiation Physics, University of Gothenburg, Göteborg, Sweden

<sup>3</sup>Biological Sciences, AstraZeneca R&D Lund, Lund, Sweden

<sup>4</sup>Lung Immunology Group, Department of Internal Medicine/Respiratory Medicine & Allergology, University of Gothenburg, Göteborg, Sweden

**Introduction:** Proton ( $^1\text{H}$ ) magnetic resonance imaging (MRI) can be utilized to quantify pulmonary edema in endotoxin-induced pulmonary inflammation and hyperpolarized (HP)  $^3\text{He}$  MRI can assess pulmonary ventilation. Neither of the methods has been applied to assess the impact of a drug on endotoxin-induced pulmonary inflammation *in vivo*. The aim of the current study was to evaluate the capability of  $^1\text{H}$  and HP  $^3\text{He}$  MRI to assess the effects of a glucocorticoid on endotoxin-induced pulmonary inflammation *in vivo*.

**Materials and Methods:** Mice were exposed to an aerosol of either saline or endotoxin (5 mg/ml) for 10 min. Half of the endotoxin-exposed mice were pretreated with a glucocorticoid (budesonide 3 mg/kg; 2 times/day) and the other half with vehicle p.o. The first budesonide treatment was administered 1 h prior to the aerosol inhalation. Forty-eight hours after the aerosol exposure, the mice were anaesthetized for subsequent imaging. Hyperpolarized  $^3\text{He}$  was administered and axial MR images of the lungs obtained. Matching  $^1\text{H}$  MR images were then acquired. The mice were sacrificed and broncho-alveolar lavage (BAL) samples were harvested to determine total and cell differential counts. **Results:** The lesion volume on both  $^1\text{H}$  and  $^3\text{He}$  MRI, were markedly increased by endotoxin exposure ( $P < 0.001$ ). Budesonide strongly reduced lesion volume ( $P < 0.001$ ). The BAL cell count correlated strongly with both  $^3\text{He}$  ( $P < 0.001$ ;  $r = 0.96$ ) and  $^1\text{H}$  lesion volumes ( $P < 0.001$ ;  $r = 0.97$ ).

**Conclusions:** Hyperpolarized  $^3\text{He}$  MRI and  $^1\text{H}$  MRI clearly visualized the preventative effect of budesonide on the impact of endotoxin on pulmonary ventilation and edema, respectively. The fact that ventilation defects on  $^3\text{He}$  MRI corresponded to findings from conventional  $^1\text{H}$  MRI, as well as to counts of BAL inflammatory cells suggests that these imaging techniques constitute promising tools for non-invasive monitoring of pulmonary inflammation *in vivo*.

**Keywords:** MRI, glucocorticoid, endotoxin, inflammation, lung function, hyperpolarized

## INTRODUCTION

Exposure to endotoxin is believed to be an important pathogenic factor not only for the course of pulmonary infections but also for severe inflammatory conditions in the lungs, such as acute respiratory distress syndrome

(ARDS), chronic obstructive pulmonary disease (COPD) and cystic fibrosis (CF).<sup>1–3</sup>

An improved understanding of endotoxin-induced pulmonary inflammation may, therefore, serve to identify novel therapeutic targets in severe lung disorders. However, the tools available for the monitoring of

Received 12 October 2009; Revised 1 December 2009; Accepted 4 December 2009

Correspondence to: Lars E. Olsson PhD, AstraZeneca R&D, Mölndal, DECS/Imaging, SE-431 83 Mölndal, Sweden.  
 E-mail: lars.e.olsson@astrazeneca.com

endotoxin-induced pulmonary inflammation have traditionally been invasive and based on broncho-alveolar lavage.<sup>4</sup>

Two previous studies have shown that proton magnetic resonance imaging (<sup>1</sup>H MRI) can be used to monitor the edema in endotoxin-induced pulmonary inflammation in rats *in vivo*.<sup>5,6</sup> Notably, <sup>1</sup>H MR imaging not only indicates disease progression but also provides regional information.

Conventional <sup>1</sup>H MR imaging only reflects the induction of edema, mucus and other morphological changes; therefore, there is a great interest in extending this morphological knowledge to include data on lung function.<sup>7</sup> Recently, hyperpolarized helium-3 (HP <sup>3</sup>He) MRI has emerged as a technique to image the air spaces in the lung of small animals and assess functional aspects such as ventilation.<sup>8</sup> The information from conventional <sup>1</sup>H MRI imaging has now also been compared with that from HP <sup>3</sup>He MRI, allowing simultaneous and non-invasive monitoring of changes in morphology and lung ventilation in endotoxin exposed mice.<sup>9</sup> Moreover, the first study to compare <sup>1</sup>H and HP <sup>3</sup>He MRI actually showed that the functional HP <sup>3</sup>He read-out was more sensitive than <sup>1</sup>H MRI imaging. It also indicated that MRI read-out was optimum at 48 h after endotoxin exposure. Until now, no studies have utilized HP <sup>3</sup>He MRI to assess the effects of a glucocorticoid on endotoxin-induced pulmonary inflammation.<sup>10</sup>

The aim of the present study was to evaluate the capability of <sup>1</sup>H and HP <sup>3</sup>He MRI to assess the effect of a glucocorticoid (budesonide) on morphology and ventilation, respectively, in endotoxin-induced pulmonary inflammation *in vivo*, utilizing cellular alterations in the broncho-alveolar space as a reference.

## MATERIALS AND METHODS

### Animal preparation

The study was approved by the local ethical committee and performed in accordance with the AstraZeneca Good Laboratory Standards. Balb/c JTac, female (Taconic M&B, Denmark) mice were used. Animal weight on delivery was 19–22 g. The mice were acclimatized in the animal facilities for at least one week before initiating the study. They were fed a standard pellet diet (R3 pellets, Lactamin) and tap water *ad libitum*. All mice were kept at the animal facilities at 50% humidity, a temperature of 21°C, and a 12/12-h light/dark cycle.

Endotoxin (lipopolysaccharide from *Pseudomonas aeruginosa*, serotype 10, L9143; Sigma-Aldrich, Sweden) was dissolved in isotonic saline (0.9% NaCl, B. Braun Medical, Sweden) to a stock solution of 5 mg/ml.

Budesonide was prepared in-house to a concentration of 300 µg/ml.<sup>10</sup> The mice were divided into three groups: two groups ( $n=8$  in each) were exposed to an aerosol of endotoxin (5 mg/ml) in inhalation boxes and one group ( $n=6$ ) was exposed to an aerosol of isotonic saline (negative control). In all cases, this exposure lasted 10 min. The endotoxin-exposed groups of mice were treated p.o. (2 times/day; approximately 0.2 ml/mouse) with either vehicle (positive control) or a glucocorticoid (budesonide: 3 mg/kg, intervention). The first p.o. treatment was administered 1 h prior to the aerosol exposure.

### MR-imaging

On the day of imaging, HP <sup>3</sup>He produced by the metastability exchange method of laser optical pumping was received from the Institut für Physik, University of Mainz, Germany. The gas was delivered in glass bulbs (~1 l at 2.7 bar, ~60% polarization). The production, storage and transport of HP <sup>3</sup>He have been described previously.<sup>11</sup>

A small animal ventilator system (ventilator and computer) dedicated to HP <sup>3</sup>He was used for gas delivery (Servicios de Electronica y Programacion Dedicados, Madrid, Spain). The ventilator has previously been described in detail.<sup>12</sup>

The MRI examination was performed 48 h after endotoxin exposure, which has been shown to be an appropriate time point for MRI read-out.<sup>9</sup> Immediately prior to the imaging, the mice were anaesthetized by Ketalar (Pfizer AB, Sollentuna, Sweden) 100 mg/kg and Rompun (Bayer AB, Göteborg, Sweden) 5 mg/kg i.p. A tracheotomy using a venflon (BD Venflon, Becton Dickinson, 20 GA, Infusion Therapy AB, Helsingborg, Sweden) as the tracheal tube was performed. Additionally, Pavulon (Organon, Teknika, Bostel, The Netherlands) 0.03 mg/kg i.p. was administered as a muscle relaxant. The mouse was connected to the ventilator and set to normal breathing with a respiratory rate of 100/min at a tidal volume of ~0.3 ml.

The MRI experiments were performed on a BioSpec 47/40 4.7 T MR scanner (Bruker BioSpin, Ettlingen, Germany) with a double tuned <sup>1</sup>H (linear) and <sup>3</sup>He (quadrature) transmit/receive coil (diameter 35 mm). The scanner was equipped with an animal bed with a circulating perfluorocarbon solution (HT170, Solvey Solexis, Bollate, Italy) to maintain body temperature during imaging.

The ventilator was set to <sup>3</sup>He delivery and 3-D images of the lungs were acquired during end-inspiration breath-hold. A 3-D gradient echo sequence was used with repetition time/echo time = 5.5/1.3 ms, field of view = 30 × 30 × 18 mm<sup>3</sup>, acquisition matrix = 64 × 64 × 12

and flip angle =  $6^\circ$ . The length of a respiratory cycle in acquisition mode was 2 s including inspiration, breath-hold ( $\sim 800$  ms) and expiration. Six cycles were needed to complete the 3-D acquisition. This was followed by an axial  $^1\text{H}$  MRI for edema assessment in which the slice positions were matched to the  $^3\text{He}$  images. Approximately eight contiguous single-slice images were acquired to cover the lung volume. A 2-D gradient echo was used with repetition time/echo time =  $7.0/2.7$  ms, slice thickness = 1.5 mm, field of view =  $30 \times 30$  mm<sup>2</sup>, acquisition matrix =  $256 \times 96$ , flip angle =  $15^\circ$ , number of averages = 30. The  $^1\text{H}$  acquisition (air) was performed with the same ventilator settings to obtain identical lung volumes during  $^3\text{He}$  and  $^1\text{H}$ . Approximately 25 respiratory cycles were needed to complete one slice ( $\sim 1$  min/slice).

### Cell counting

Immediately after the imaging procedure, the animals were sacrificed and a BAL was performed by cannulation of the trachea and administration of isotonic phosphate-buffered saline (PBS, Gibco, Life Technologies, Sweden) for 2 min using 20 cm H<sub>2</sub>O pressure. Fluid was collected in a tube on ice. The procedure was repeated twice. The lavage was centrifuged (14,400 g, 10 min,  $4^\circ\text{C}$ ), supernatant removed and the cell pellet was resuspended in isotonic PBS. The total cell number was counted manually using a Burkert's chamber in the presence of Turk's staining solution. The total number of cells per milliliter was assessed. Slides were made from cytopsin (Shandon III, 5000 g, 3 min) and stained with May-Grünwald-Giemsa. The cell differentiation number was based on percentage from 300 counted cells/slide using standard morphological criteria to identify cell types.

### Image and data analysis

The  $^3\text{He}$  and  $^1\text{H}$  images were analyzed in a blinded manner (*i.e.* by one experienced reader with no knowledge of which group the animals were in). In the axial images, the number of lesions ( $^3\text{He}$ , ventilation defect;  $^1\text{H}$ , edema) were counted and their areas were measured manually in each slice (ParaVision v.4 software; Bruker BioSpin, Ettlingen, Germany). The volume of the lesions was calculated by multiplying the lesion area by the slice thickness. A summation over all slices in each animal resulted in total  $^3\text{He}$  and  $^1\text{H}$  MRI lesion volumes per mouse, respectively. The method has been described in detail previously.<sup>9</sup> The  $^3\text{He}$  and  $^1\text{H}$  MR images were analyzed independently from each other and on separate occasions to avoid bias.

The statistical significance of the differences between groups and time points were calculated using a *t*-test with two-tailed distribution and two-sample unequal variance. In the figures, the significance is marked according to the following criteria: \*\*\* $P < 0.001$ ; \*\* $P < 0.01$ ; \* $P < 0.05$ . The Pearson correlation coefficient was used as a measure of data correlation.

## RESULTS

The imaging protocol described covered the entire lung volume for both  $^3\text{He}$  and  $^1\text{H}$  MRI (Fig. 1).  $^3\text{He}$  images of the lungs of animals in the negative control group (healthy mice exposed to saline aerosol) were characterized by a sharp delineation of the lungs and homogeneous filling of gas with the exception of areas corresponding to major vessels. The corresponding  $^1\text{H}$  images showed dark lungs with the only signal coming from large blood vessels (Fig. 1 and Fig. 2A).  $^3\text{He}$  images of mice in the positive control group (endotoxin-exposed and vehicle-treated mice) showed severe ventilation defects with corresponding hyperintense areas on the  $^1\text{H}$  images (Fig. 2B). Images of mice in the budesonide intervention group (endotoxin-exposed and budesonide-treated) were largely free from the ventilation defects on the  $^3\text{He}$  images and the lesions on the  $^1\text{H}$  images (Fig. 2C).

The volume of lesion for both  $^3\text{He}$  and  $^1\text{H}$  MR imaging showed a statistically significant difference ( $P < 0.001$ ) between the negative control group and the positive control group (Fig. 3). Intervention with budesonide caused a significant reduction ( $P < 0.001$ ) in lesion volume in the endotoxin-exposed mice. The efficacy of this reduction was 91% and 85%, measured by  $^3\text{He}$  and  $^1\text{H}$  MRI, respectively. There was no statistically significant difference in the volume of ventilation defects measured by  $^3\text{He}$  MRI between the negative control group and the budesonide intervention group, whereas intervention did not return the  $^1\text{H}$  MRI lesion volume completely to control levels ( $P < 0.05$ ).

The manually measured lung volumes were significantly ( $P < 0.001$ ) larger on  $^3\text{He}$  images than on  $^1\text{H}$  images (Table 1). Correspondingly, the volume of the lesions was larger ( $P < 0.01$ ) on the  $^3\text{He}$  images. There was no significant difference in the number of lesions for  $^1\text{H}$  and  $^3\text{He}$  MRI. The lesions measured as a fraction of the lung volume were not significantly different for  $^1\text{H}$  and  $^3\text{He}$  MRI (Fig. 4 and Table 1).

The total number of BAL cells was significantly reduced by budesonide treatment ( $P < 0.001$ ), with an efficacy of 80%. The majority of collected BAL cells were neutrophils (87% of the total number) and treatment efficacy on the inhibition of their number was 83% ( $P < 0.001$ ). The number of lymphocytes was also reduced significantly ( $P < 0.001$ ), with an efficacy

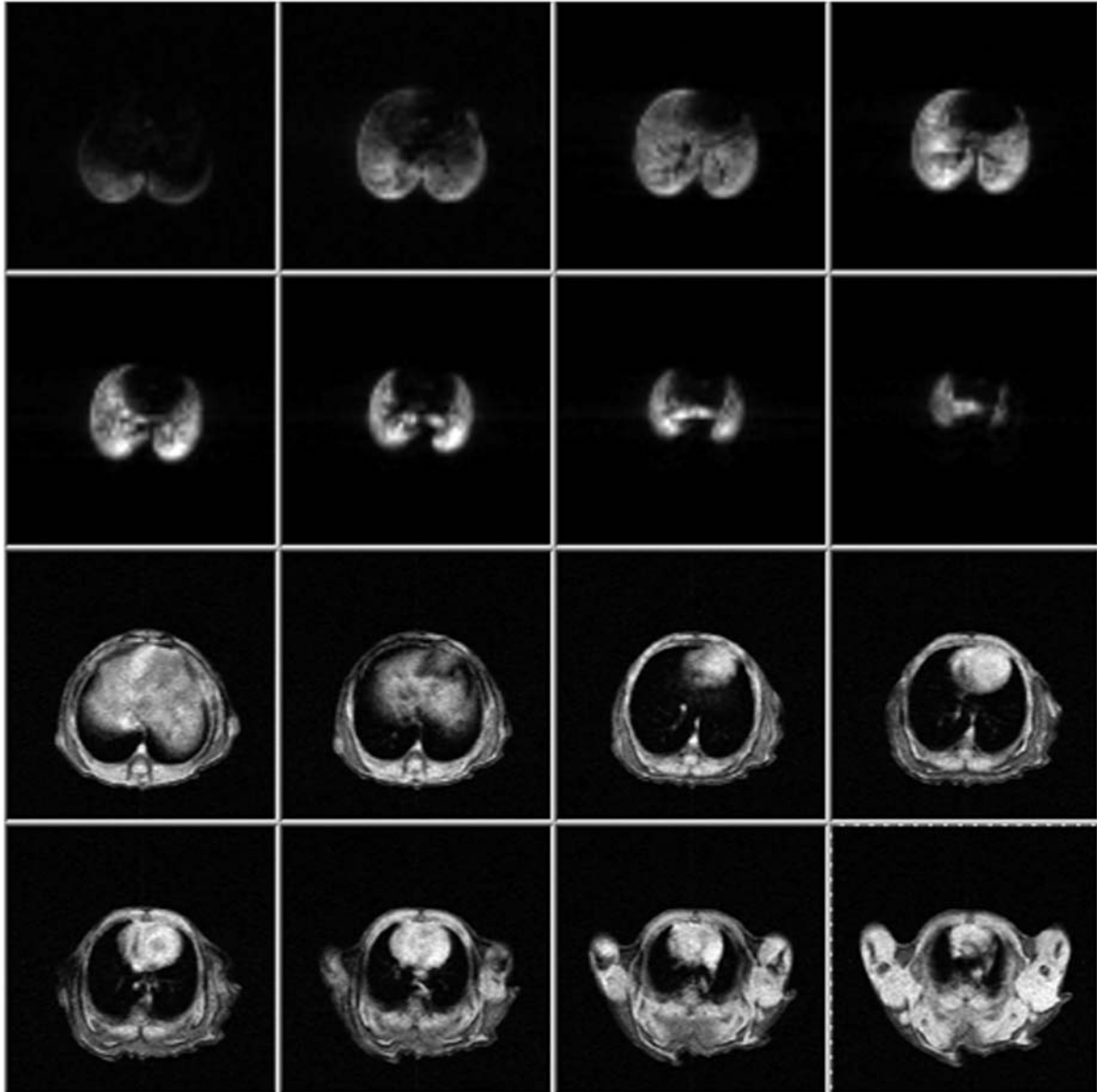


**Fig. 1.** Axial pulmonary MRI on the thorax of a saline-exposed mouse. HP  $^3\text{He}$  MRI depicting ventilation (upper two rows) and matching  $^1\text{H}$  MRI (lower two rows).

of 90%. A tendency for budesonide treatment to reduce macrophage numbers was observed but it did not reach statistical significance (Fig. 5).

There was a strong correlation between the lesion volumes found by either  $^3\text{He}$  MRI or  $^1\text{H}$  MRI and the neutrophils, lymphocytes and the total BAL cell numbers (Fig. 6 and Table 2). The corresponding correlations for macrophages were modest.

#### DISCUSSION

In the present study, we demonstrate that  $^1\text{H}$  and  $^3\text{He}$  MRI can detect the preventative effects of the

glucocorticoid budesonide on endotoxin-induced pulmonary inflammation in mice *in vivo*. More specifically, treatment with budesonide prevented the formation of lung edema and improved ventilation in the small airways. These findings correlated with the inhibitory effects of budesonide on the number of inflammatory cells in BAL fluid. Notably, the preventative effects of a glucocorticoid on endotoxin-exposed rodents have been characterized previously,<sup>10,13</sup> but never before with MRI as a read-out; therefore, the present study is the first using MRI to monitor the impact of a glucocorticoid on endotoxin-induced pulmonary inflammation *in vivo*.

Conventional  $^1\text{H}$  MRI has been applied as a read-out in disease models other than LPS, for example in

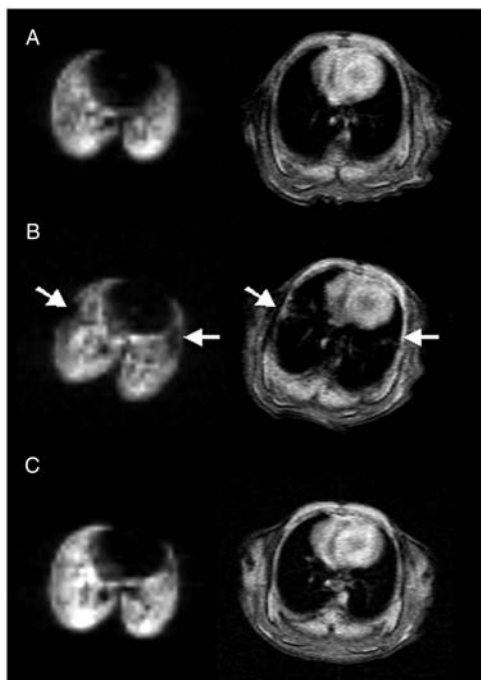


**Fig. 2.** One slice displayed out of a full pulmonary coverage (HP  $^3\text{He}$  left,  $^1\text{H}$  right). (A) Negative control (saline-exposed mouse, Control); (B) positive control (endotoxin-exposed mouse treated with saline, Vehicle); (C) intervention (endotoxin-exposed mouse treated with budesonide, Budesonide). Arrows indicate lesions. The images were acquired 48 h after the saline/endotoxin exposure.

sensitized rats challenged with ovalbumin, with and without budesonide treatment.<sup>14–16</sup> Interestingly, the effect of budesonide treatment on the edema in these studies measured by  $^1\text{H}$  MRI was similar to that observed in the current study on endotoxin-exposed mice.

Hyperpolarized  $^3\text{He}$  has been used to characterize several other models of pulmonary disorders, such as the elastase model of emphysema, methacholine-induced bronchoconstriction and ozone-induced bronchial hyper-reactivity.<sup>17–19</sup> Hyperpolarized  $^3\text{He}$  was recently applied to characterize endotoxin-induced pulmonary inflammation in mice *in vivo*,<sup>9</sup> but our current study is the first to use this method to show the impact of a drug intervention in this context.

The findings from both  $^1\text{H}$  and  $^3\text{He}$  MRI in the present study were closely correlated to cellular markers of inflammation in the broncho-alveolar space. This correlation is higher than that found previously in endotoxin-exposed rats monitored with a  $^1\text{H}$  MRI read-out.<sup>15</sup> Moreover, a similar correlation between  $^1\text{H}$  MRI and inflammatory markers, as in the present study, has been found in rats exposed to ovalbumin.<sup>15</sup> In all of the mentioned studies, including our current one, the lowest correlation was found between MRI and the macrophage concentration in the BAL sample.

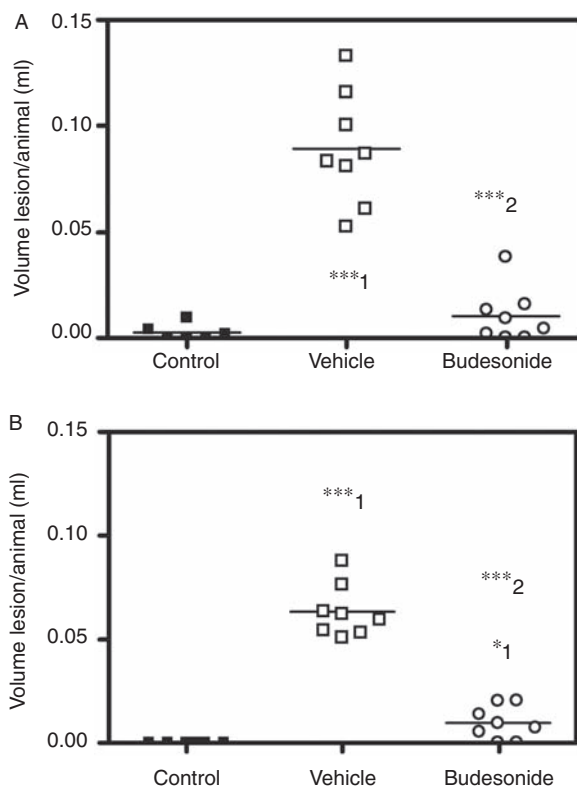


**Fig. 3.** The lesion volumes assessed by (A) HP  $^3\text{He}$  MRI and (B)  $^1\text{H}$  MRI. For the *t*-test, index 1 refers to statistically significant difference compared with negative control (saline-exposed mouse, Control) and index 2 refers to statistically significant difference compared with positive control (endotoxin-exposed mouse treated with saline, Vehicle).

**Table 1.** Correlation between  $^3\text{He}$  and  $^1\text{H}$  MRI. The *t*-test was made on original data

	Ratio $^3\text{He}/^1\text{H}$	<i>P</i> -value <i>t</i> -test
Lung volume	1.39	<0.001
Number of lesions	1.03	ns
Lesion volume/animal	1.44	<0.01
Lesion fraction of lung vol.	1.04	ns

The volumes of the lungs and lesions measured by  $^3\text{He}$  MRI were larger than from the  $^1\text{H}$  MRI. Although, the ventilator was set to the same tidal volumes for  $^1\text{H}$  and  $^3\text{He}$ , the channels were separately controlled. Therefore, there is a possibility that the tidal volumes differ, but this is unlikely to explain the full extent of the difference. There were several differences in the way the volumes were outlined on the images. The regions for assessing the lung volume on the  $^3\text{He}$  images encompass the lung, but the regions on  $^1\text{H}$  images were drawn inside the

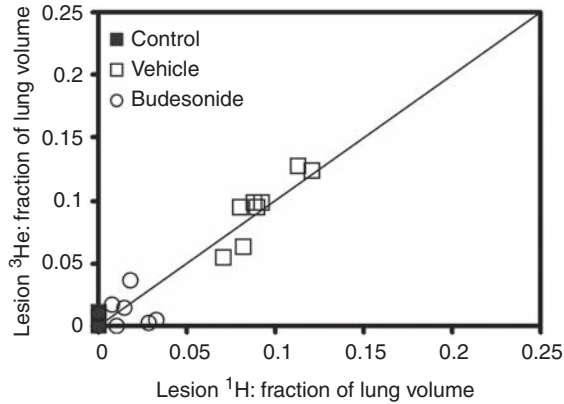


**Fig. 4.** The correlation between the lesion volume measured by HP  $^3\text{He}$  MRI and  $^1\text{H}$  MRI (the line represents the line of identity).  $P < 0.001$ ;  $r = 0.83$ .

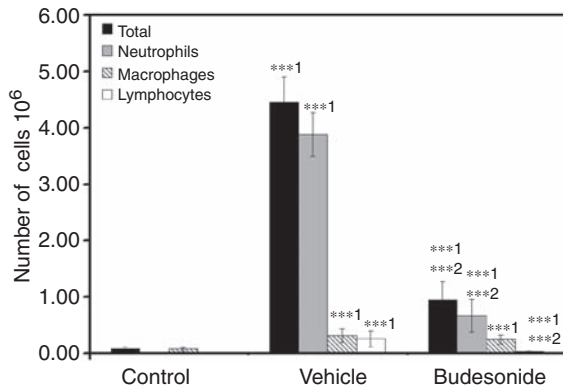


**Fig. 5.** The total count for inflammatory BAL cells and the subpopulation counts of these cells: neutrophils, macrophages and lymphocytes. The error bars indicate  $\pm$  SEM. For the  $t$ -test, index 1 refers to statistically significant difference compared with negative control (saline-exposed mouse, Control) and index 2 refers to statistically significant difference compared with positive control (endotoxin-exposed mouse treated with saline, Vehicle).

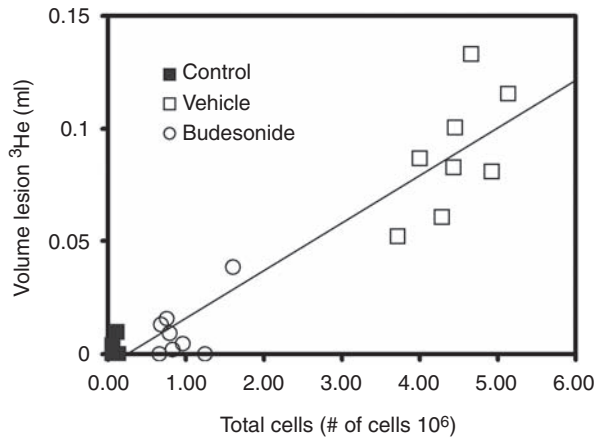


**Fig. 6.** The correlation between total count for inflammatory BAL cells and the lesion volume measured by HP  $^3\text{He}$  MRI.  $P < 0.001$ ;  $r = 0.96$ .

**Table 2.** Correlations between counts of BAL inflammatory cells and  $^3\text{He}$  and  $^1\text{H}$  MRI data (lesion volume)

	$^3\text{He}$ data		$^1\text{H}$ data	
	Correlation	$P$ -value	Correlation	$P$ -value
Total cells	0.956	<0.001	0.969	<0.001
Neutrophils	0.958	<0.001	0.970	<0.001
Macrophages	0.552	<0.01	0.560	<0.01
Lymphocytes	0.840	<0.001	0.855	<0.001

thorax wall. Therefore, there was a tendency that the volume of the  $^3\text{He}$  images were overestimated compared to  $^1\text{H}$  images. The bronchi and vessels are included in the measured volume from the  $^3\text{He}$  images and were, therefore, also included in the  $^1\text{H}$  images. Due to partial volume effects and motion, the outline of the diaphragm was a challenging task on the  $^1\text{H}$  images resulting in some uncertainty. We conclude that the greater lesion volumes measured on  $^3\text{He}$  compared to  $^1\text{H}$  are largely due to the operator's tendency to draw the edges of the region of interest in different positions on the two image types, especially since there is no difference if the lesions of  $^3\text{He}$  and  $^1\text{H}$  are counted as the fraction of lung volume.

The results from  $^3\text{He}$  and  $^1\text{H}$  MRI were similar in many respects, including the clear detection of glucocorticoid impact on pulmonary inflammation. In the endotoxin-exposed mice, budesonide decreased the lesion volume by 91% in  $^3\text{He}$  MRI and by 85% in  $^1\text{H}$  MRI; this corresponds very well to the 80–90% decrease of BAL inflammatory cells in the same mice. Notably, the precise lesion volume obtained after budesonide treatment was very similar in both types of MRI. However, the volume of lesion detected by  $^1\text{H}$  MRI in the budesonide intervention group was still different from the negative control group whereas this was not the case for ventilation defects measured with  $^3\text{He}$  MRI. This may be the result of a larger variation in ventilation defect volume in the negative control group than was the case for  $^1\text{H}$  MRI, possibly caused by small non-ventilated areas detected by  $^3\text{He}$  MRI in a few mice. Ventilation defects in healthy individuals, as in the individuals in the negative control group, are not unusual and have been observed previously in both mice and in humans examined with hyperpolarized  $^3\text{He}$  MRI.<sup>9,20</sup> Mechanical ventilation can also cause ventilation defects. However, these effects only arise after hours of mechanical ventilation. In the present study, the ventilation was less than 30 min, and the  $^3\text{He}$  MRI was performed during the first 15 min. We do not expect that this procedure will cause significant lung injury, which is also supported by the normal levels of cells in the BAL. Nevertheless, the need for mechanical ventilation to administer the gas is still a considerable disadvantage

for  $^3\text{He}$  MRI due to its invasive nature. Recent studies suggest that  $^3\text{He}$  MRI can be accomplished for freely breathing animals, thereby allowing longitudinal studies with repeated measurements of individual subjects, which obviously would be of great benefit especially in drug studies.<sup>21</sup>

As judged from our current results on endotoxin-induced pulmonary inflammation in a mouse model, both assessment of pulmonary edema with  $^1\text{H}$  MRI and of pulmonary ventilation with HP  $^3\text{He}$  MRI can be considered as appropriate read-outs *in vivo*. No particular advantage was found for HP  $^3\text{He}$  MRI as the non-ventilated areas in the lungs reflect the degree of edema at the same location. This relationship does not necessarily hold true for disease models and drug treatments other than the current ones. Also,  $^3\text{He}$  MRI offers many other read-outs, which have not been within the scope of the present study, such as measurement of apparent diffusion coefficient or regional partial oxygen pressure.<sup>8,22</sup> It remains to be shown what these methods add to different animal models of pulmonary disease compared to simple ventilation. Thus, it is for future studies to demonstrate the advantage of the complementary nature of the HP  $^3\text{He}$  ventilation and  $^1\text{H}$  edema assessments in pulmonary inflammation.

### CONCLUSIONS

Hyperpolarized  $^3\text{He}$  and  $^1\text{H}$  MRI were successfully applied to detect the preventative effect of a glucocorticoid on endotoxin-induced pulmonary inflammation *in vivo*. The altered ventilation measured with  $^3\text{He}$  MRI corresponded very well with the detection of edema with conventional  $^1\text{H}$  MRI, as well as with counts of inflammatory cells in the broncho-alveolar space. Our current study suggests that the tested MRI techniques constitute promising tools for non-invasive monitoring of pulmonary inflammation *in vivo*.

### ACKNOWLEDGEMENT

The authors would like to express their gratitude to Prof. Heil and his colleagues at the University of Mainz and to Dr Perez de Alejo at the University of Madrid for their valuable scientific and technical support of this study. We also thank Dr Miller-Larsson at AstraZeneca R&D Lund for her constructive criticism during the preparation of this manuscript.

### REFERENCES

1. Alridge AJ. Role of the neutrophil in septic shock and the adult respiratory distress syndrome. *Eur J Surg* 2002; **168**: 204–214.

2. Eduard W, Pearce N, Douwes J. Chronic bronchitis, COPD, and lung function in farmers: the role of biological agents. *Chest* 2009; **136**: 716–725.
3. Pier GB. *Pseudomonas aeruginosa* lipopolysaccharide: a major virulence factor, initiator of inflammation and target for effective immunity. *Int J Microbiol* 2007; **297**: 277–295.
4. Wright JL, Chung A. Animal models of COPD: barriers, successes, and challenges. *Pulmon Pharm Ther* 2008; **21**: 696–698.
5. Beckmann N, Tigani B, Sugar R, Jackson AD. Noninvasive detection of endotoxin-induced mucus hypersecretion in rat lung by MRI. *Am J Physiol* 2002; **283**: L22–L30.
6. Quintana HK, Cannet C, Schaeublin E *et al.* Identification with MRI of the pleura as a major site of the acute inflammatory effects induced by ovalbumin and endotoxin challenge in the airways of the rat. *Am J Physiol* 2006; **291**: L651–L657.
7. Chen BT, Brau ACS, Johnson GA. Measurement of regional lung function in rats using hyperpolarized  $^3\text{He}$  dynamic MRI. *Magn Reson Med* 2003; **49**: 78–88.
8. Dugas JP, Garbow JR, Kobayashi DK, Conradi MS. Hyperpolarized  $^3\text{He}$  MRI of mouse lung. *Magn Reson Med* 2004; **52**: 1310–1317.
9. Olsson LE, Smailagic A, Önnervik PO, Hockings PD.  $^1\text{H}$  and hyperpolarized  $^3\text{He}$  MR imaging of mouse with LPS induced inflammation. *J Magn Reson Imag* 2009; **29**: 977–981.
10. Jansson AH, Eriksson C, Wang XD. Effects of budesonide and *N*-acetylcysteine on acute lung hyperinflation, inflammation and injury in rats. *Vasc Pharmacol* 2005; **43**: 101–111.
11. van Beek EJR, Schmiedeskamp J, Wild JM *et al.* Hyperpolarized 3-helium MR imaging of the lungs: testing the concept of a central production facility. *Eur Radiol* 2003; **13**: 2583–2586.
12. Perez De Alejo R, Ruiz-Cabello J, Palmira V *et al.* A fully MR-compatible animal ventilator for special-gas mixing applications. *Conc Magn Reson* 2005; **26B**: 93–103.
13. Miller Larsson A, Jansson P, Runström A, Brattsand R. Prolonged airway activity and improved selectivity of budesonide possibly due to esterification. *Am J Respir Crit Care Med* 2000; **162**: 1455–1461.
14. Beckmann N, Tigani B, Ekatothramis D, Borer R, Mazzoni L, Fozard JR. Pulmonary edema induced by allergen challenge in the rat: noninvasive assessment by magnetic resonance imaging. *Magn Reson Med* 2001; **45**: 88–95.
15. Tigani B, Schaeublin E, Sugar R, Jackson AD, Fozard JR, Beckmann N. Pulmonary inflammation monitored noninvasively by MRI in freely breathing rats. *Biochem Biophys Res Commun* 2002; **292**: 216–221.
16. Tigani B, Cannet C, Zurbrugg S *et al.* Resolution of the edema associated with allergic pulmonary inflammation in rats assessed noninvasively by magnetic resonance imaging. *Br J Pharmacol* 2003; **140**: 239–246.
17. Emami K, Cadman RV, Woodburn JM *et al.* Early changes of lung function and structure in an elastase model of emphysema – a hyperpolarized  $^3\text{He}$  MRI study. *J Appl Physiol* 2008; **104**: 773–786.
18. Crémillieux Y, Servais S, Berthezène Y *et al.* Effects of ozone exposure in rat lungs investigated with hyperpolarized  $^3\text{He}$  MRI. *J Magn Reson Imag* 2008; **27**: 771–776.
19. Mosbah K, Crémillieux Y, Adeleine P *et al.* Quantitative measurements of regional lung ventilation using helium-3 MRI in a methacholine-induced bronchoconstriction model. *J Magn Reson Imag* 2006; **24**: 611–616.
20. Mata J, Altes T, Knake J, Mugler III J, Brookeman J, de Lange E. Hyperpolarized  $^3\text{He}$  MR imaging of the lung: effect of subject

- immobilization on the occurrence of ventilation defects. *Acad Radiol* 2008; **15**: 260–264.
21. Stupar V, Canet-Soulas E, Gaillard S, Alsaïd H, Beckmann N, Crémillieux Y. Retrospective cine  $^3\text{He}$  ventilation imaging under spontaneous breathing conditions: a non-invasive protocol for small-animal lung function imaging. *NMR Biomed* 2007; **20**: 104–112.
  22. Fischer MC, Kadlecěk S, Yu J *et al.* Measurements of regional alveolar oxygen pressure using hyperpolarized  $^3\text{He}$  MRI. *Acad Radiol* 2005; **12**: 1430–1439.